Food & Function

Accepted Manuscript

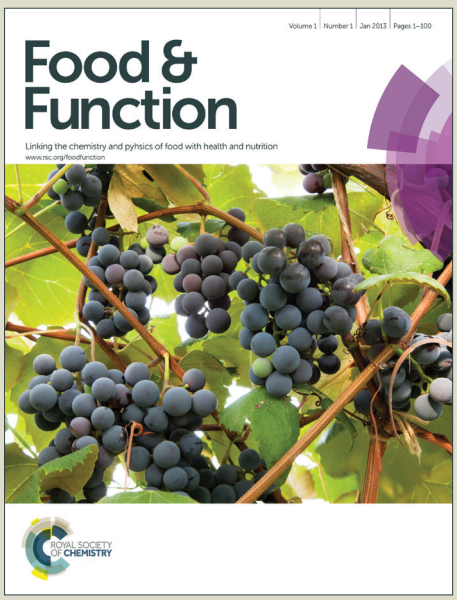

This is an *Accepted Manuscript*, which has been through the Royal Society of Chemistry peer review process and has been accepted for publication.

Accepted Manuscripts are published online shortly after acceptance, before technical editing, formatting and proof reading. Using this free service, authors can make their results available to the community, in citable form, before we publish the edited article. We will replace this *Accepted Manuscript* with the edited and formatted *Advance Article* as soon as it is available.

You can find more information about *Accepted Manuscripts* in the Information for Authors.

Please note that technical editing may introduce minor changes to the text and/or graphics, which may alter content. The journal's standard Terms & Conditions and the Ethical guidelines still apply. In no event shall the Royal Society of Chemistry be held responsible for any errors or omissions in this *Accepted Manuscript* or any consequences arising from the use of any information it contains.

ROYAL SOCIETY OF CHEMISTRY

www.rsc.org/foodfunction

In vitro fermentation of chewed mango and banana: Particle size, starch and vascular fibre effects

Dorrain Y. Low[1], Barbara A. Williams[1], Bruce R. D'Arcy[2], Bernadine M. Flanagan[1], Michael J. Gidley[1]

[1]*ARC Centre of Excellence in Plant Cell Walls, Centre for Nutrition and Food Sciences, Queensland Alliance for Agriculture and Food Innovation, The University of Queensland, 4072, Australia.*

[2]*School of Agriculture and Food Sciences, The University of Queensland, 4072, Australia.*

**Corresponding author: Michael J. Gidley. Address: Hartley Teakle Building, The University of Queensland, 4072, Australia. Email: m.gidley@uq.edu.au. Tel: +61 7 3365 2145. Fax. +61 7 3365 1177.*

Table of contents entry

Colour graphic:

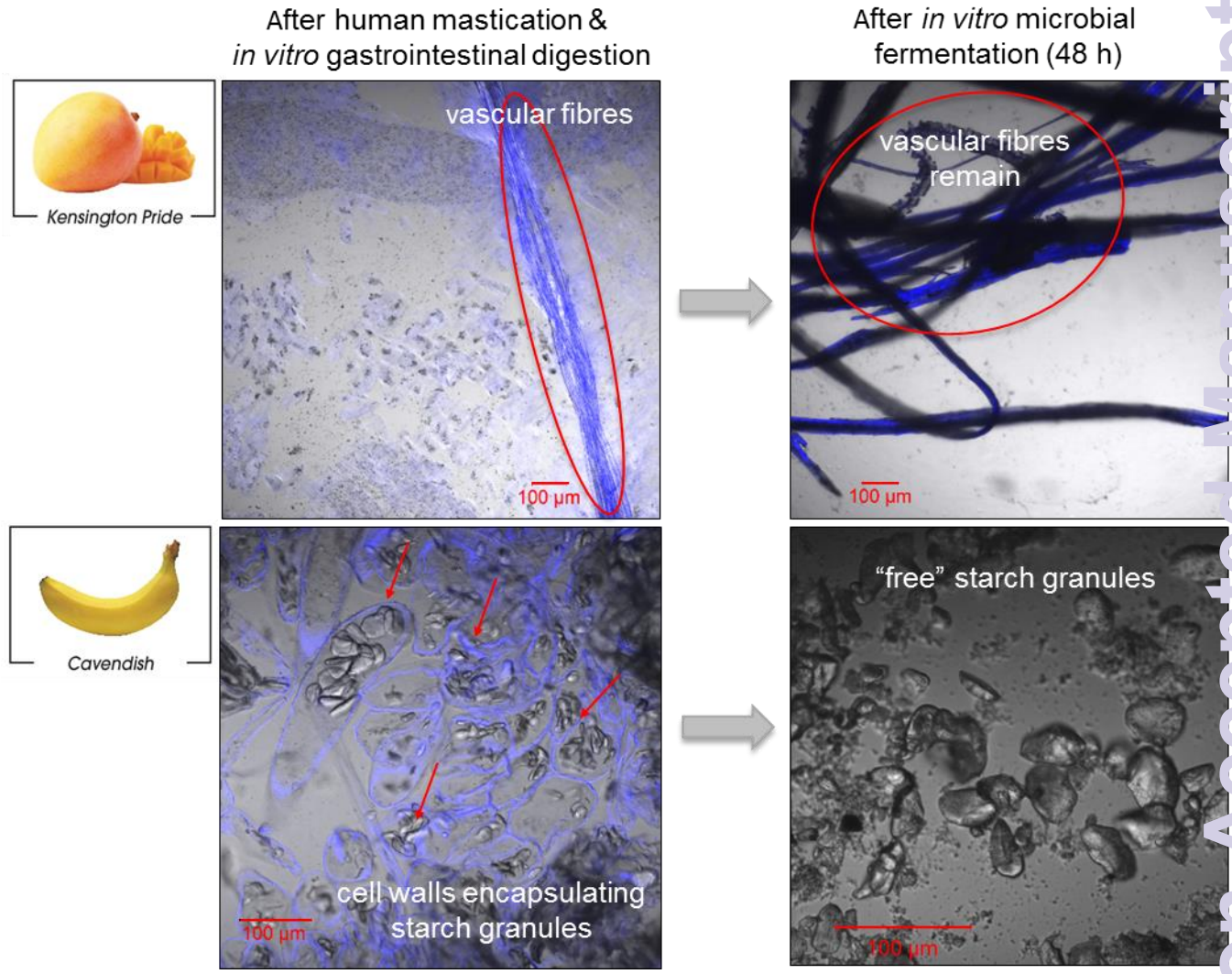

The presence of resistant starch in chewed banana and vascular fibres in chewed mango, have greater effects on microbial fermentation kinetics than particle size.

Abstract

Fruits (and vegetables) contain cellular structures that are not degraded by human digestive enzymes. Therefore, the structure of the insoluble fraction of swallowed fruits is mostly retained until intestinal microbial fermentation. *In vitro* fermentation of mango and banana cell structures, which survived *in vivo* mastication and *in vitro* gastrointestinal digestion, were incubated with porcine faecal inoculum and showed intensive metabolic activity. This included degradation of cell walls, leading to the release of encapsulated cell contents for further microbial metabolism. Production of cumulative gas, short chain fatty acids and ammonia were greater for mango than for banana. Microscopic and spectroscopic analyses showed this was due to a major fermentation-resistant starch fraction present in banana, that was absent in mango. This study demonstrated distinctive differences in the fermentability of banana and mango, reflecting a preferential degradation of (parenchyma) fleshy cell walls over resistant starch in banana, and the thick cellulosic vascular fibres in mango.

Keywords: microbial fermentation, gas production, mango, banana, resistant starch, cellulose.

1. Introduction

In vivo investigations of dietary polysaccharide fermentation in the human colon can be challenging due to inaccessibility, inconsistency and limitations of dietary control for human volunteers [1]. There is continued interest in the development of relevant *in vitro* models for the digestive process, but uncertainty exists as to how to best to represent the unit processes involved. Non-invasive *in vitro* colonic fermentation models can be used to monitor differences in substrate fermentability before and after gastrointestinal digestion [2, 3], and to elucidate the potential role of microbiota in the metabolism of partially and/or non-digestible components of the diet such as dietary fibre. *In vitro* colonic models involving faecal or caecal microbiota of human, rat and pig have proved useful for investigating metabolic processes mediated by intestinal microbiota [4]. For comparative purposes, it is important that the microbiota used as an inoculum is from a well-defined source.

Selected fruits and vegetables have been examined *in vitro* using colonic fermentation techniques [5-9]. The volume of gas produced as a result of fermentation acts as an indicator of potential fermentability of the substrate in response to a controlled microbial population. The predominant gas (CO_2) is derived from primary fermentation and the reaction of acidic fermentation end-products with basic bicarbonate ions [10, 11]. Short chain fatty acids (SCFA) such as acetic, propionic and butyric acids are major products of carbohydrate fermentation, and are known to be beneficial in terms of energy contribution and health [12], whereas ammonia (NH_3), one of the end-products of protein and peptide fermentation [13], has potentially negative effects on the long-term health of colonic epithelial cells [14].

Previous authors have used a variety of pre-treatments for fruits and vegetables in *in vitro* digestion studies including milling or grinding with hammer mills, blenders, mortars and pestles [15-17], and homogenisation [18-21], often preceded by air-drying [22] or lyophilisation [23, 24]. In addition, wet liquid samples such as purees or juices have been prepared [20, 25]. However, these high-shear techniques result in the disintegration and collapse of most of the cellular structures, which does not necessarily simulate the human mastication process, consequently leading to significant overestimates in phytonutrient bioaccessibility. For example, the carotenoid bioaccessibility of pureed mango is significantly higher and twice that of *in vivo* masticated mango fractions of varying particle sizes [26].

The aim of this study was to investigate the fermentation kinetics and end-products of fresh mango and banana flesh using a standardised batch fermentation model (with a

faecal inoculum obtained from pigs fed a well-defined diet) after *in vivo* human mastication and *in vitro* digestion processing. In this context, the fruits were prepared in such a way that the state and condition of these samples at the start of colonic fermentation were as physiologically comparable as possible to the microstructures achieved at the beginning of the colon during human consumption, *i.e.* using minimal artificial processing. Following mastication, samples were size-fractionated to allow comparison of the effect of particle size on subsequent fermentation behaviour.

2. Results

2.1. Fermentation kinetics of mango and banana

The cumulative gas production profiles (DMCV) for mango and banana are shown in Fig 1. Measured data points fitted well to mathematical predictions of Groot's model [27] for all substrate types except for the unfractionated mango where the measured gas values were higher than the predicted curve. A comparison of replicates (n=4 per particle size per fruit) indicated that the sample bottles 1, 2, 7, 11, 15 and 17 behaved as outliers (Fig S1, supplementary data); therefore, these data were excluded from Proc GLM analysis to avoid false means because the high variation in raw data contributed to exaggerated estimates for $T_{1/2}$, TR_{max} and R_{max} values based on the curve fitting results. Each substrate fraction consisted of a range of particle sizes, for example, the 2.8 mm fraction contains masticated mango or banana particles ranging from 2.8-5.6 mm while the 1 mm fraction consists of particles from 1-2.8 mm and the 0.075 mm fraction consists of particles from 0.075-1 mm. Therefore, there might be heterogeneity in each fraction as a result of the biological mastication process and/or during sub-sampling of these heterogeneous samples into individual bottles as replicates, leading to accumulated variation in individual bottles. Updated $DMCV_{48}$ means are shown in Fig 1A and 1B. Interestingly, there was an apparent opposite trend for mango and banana as a function of particle size, although the absolute differences in gas production volume between particle sizes were small. An inverse relationship between particle size and gas production was observed for mango, in contrast to banana where unfractionated and larger banana particles showed faster and more extensive gas production. The higher distribution of larger bolus particles relative to smaller particles in the unfractionated banana (mixture of particle sizes) is likely to have contributed to the higher gas production volume. All substrates started with an initial lag phase of 2-6 h, suggesting an adaption time is required for physical adhesion of cellulolytic microbial species to the fibrous plant cell wall components [28, 29].

Mango was more readily fermentable and to a greater extent, as the total gas production for mango (440 mL/g DM) was significantly greater than for banana (113 mL/g DM) (P<0.0001) (Table S1, supplementary data). Mango reached its maximum rate of gas production (R_{max}=17 mL/h) at 19 h while banana only reached its maximum rate (R_{max}=3 mL/h) after 31 h, reflecting a significant fruit effect (P<0.0001). In addition, the half-time to reaching asymptotic gas production differed significantly between mango and banana (25 h and 54 h respectively, P<0.0001). Neither the end-point gas production (48 h) nor R_{max} were significantly different between particle sizes (P>0.05), but $T_{1/2}$ and TR_{max} occurred significantly later for the 0.075 mm and 2.8 mm particles (P=0.02 and P=0.0002 respectively). The effects of fruit type and particle size, and any interactions of the fermentation kinetic parameters ($DMCV_{48}$, $T_{1/2}$, TR_{max}, R_{max}), are shown in Table S1. In banana, the $T_{1/2}$ and R_{max} of 1 mm particles were not significantly different (P>0.05) from the other particle sizes. However, the time at which the 1 mm particles reached the maximum rate of gas production (TR_{max} = 19 h) was significantly shorter (P<0.0001) than the other sizes (TR_{max} = 29-41 h) (Table S2), suggesting substrate heterogeneity from the mastication process and/or from mixing complications before sub-sampling. As fermentation of the substrates apparently would have extended beyond 48 h, gas production asymptotes were extrapolated rather than observed (Fig 1), particularly for banana.

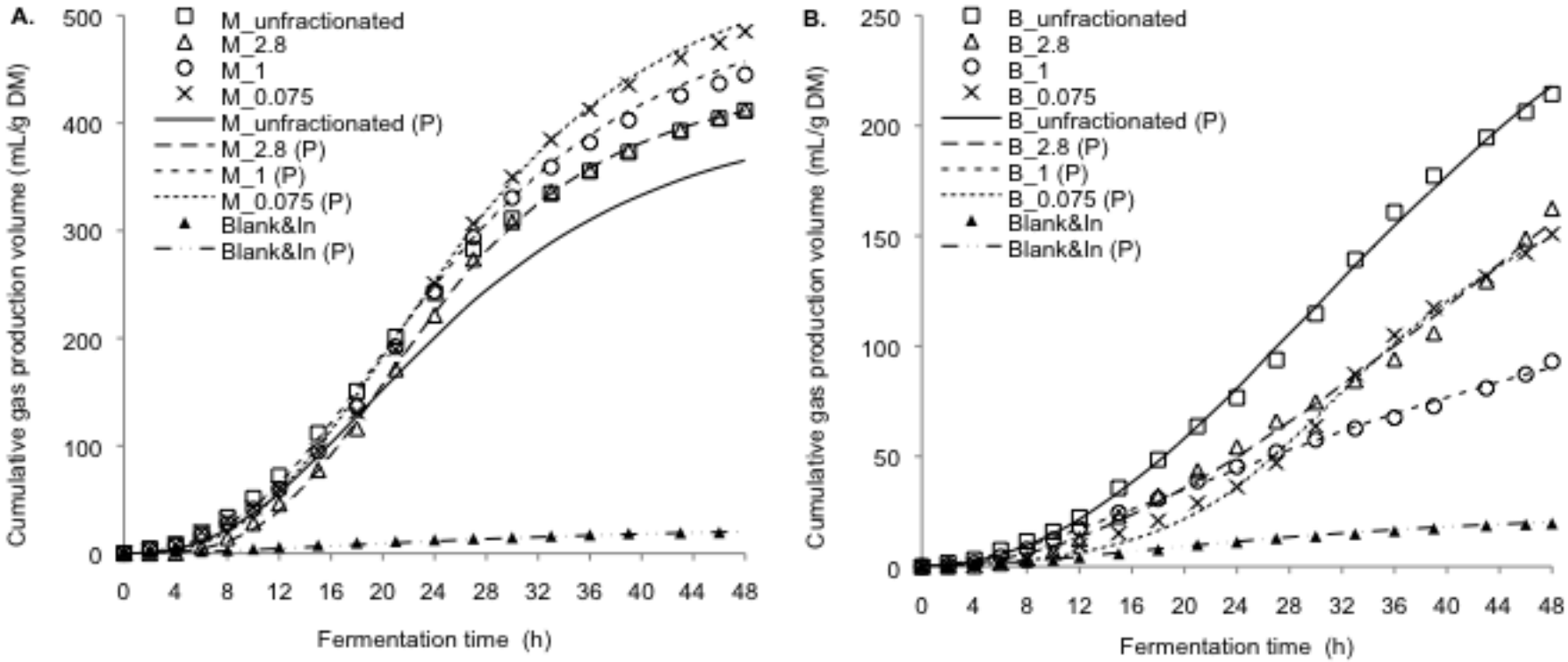

Figure 1. (Measured) cumulative gas production volume (DMCV) profiles of masticated (A) mango and (B) banana data points (□, Δ, O, x) and experimental blank (▲), and fitted monophasic curve (P) predictions (—, – – –, - - -, ---, – ¨ –) according to Groot's mathematical model (n=4 for each particle size- unfractionated, 2.8 mm, 1 mm, 0.075 mm). DMCV values have been corrected for dry matter content per substrate fermentation bottle during 48 h microbial fermentation *in vitro*. Data is expressed as means±standard deviation. Note the different y-axis scales for the two profiles. M, mango; B, banana; Blank&In, blank containing only inoculum and medium.

2.2. pH, SCFA, BCR and NH_3 in mango and banana

At the end of fermentation, the pH values for mango and banana ranged from 6.15-6.55 (Table S1). There was no significant difference (*P*>0.05) in pH either due to fruit or particle size, indicating [30, 31]that the buffering capacity of the medium was sufficient for the fermentations taking place.

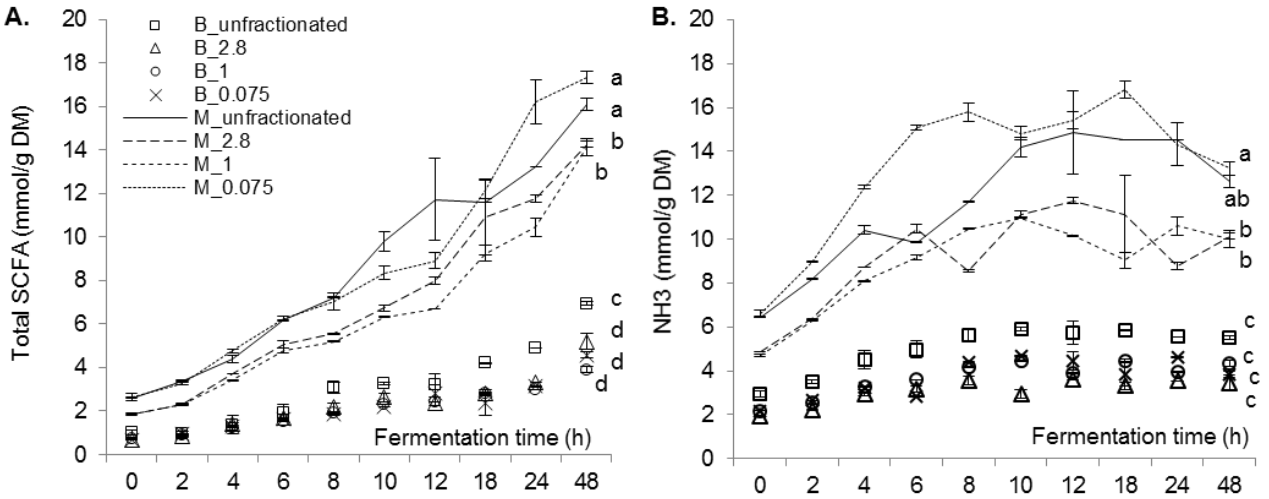

Figure 2. (A) Total short chain fatty acids (SCFA) and (B) ammonia (NH_3) production profiles of mango (□, Δ, O, x) and banana (—, – – –, - - -, ---) particles (n=4 for each particle size- unfractionated, 2.8 mm, 1 mm, 0.075 mm) during 48 h microbial fermentation *in vitro*. SCFA and NH_3 concentrations are reported as mmol/g dry matter (DM). Data are expressed as means±standard deviation. [a,b,c,d] Different letters within substrates denote significance differences for end-point values (48 h) at *P*<0.05. M, mango; B, banana.

Changes in total SCFA and NH_3 concentrations with time are shown in Fig 2. All mango fractions consistently produced significantly larger amounts of total SCFA in comparison to banana (*P*<0.0001), which is in agreement with the retarded fermentability of banana as evidenced by the lower volume and rate of gas production. The total SCFA concentration initially started from 0.7 mmol/g and showed a gradual increase over 48 h for both fruit types. Small but significant particle size effects were observed for the total SCFA (*P*<0.0001). The unfractionated and smallest particles (0.075 mm) produced significantly higher total SCFA (12.4 and 11.9 mmol/g DM) than the 2.8 mm and 1 mm particles (10.4 and 9.6 mmol/g DM). This trend was also observed for the major individual SCFA- acetic, butyric and propionic acids (Table S1).

NH_3 concentrations were at least two-fold higher for all mango particle sizes compared to banana (*P*=0.0026). Similarly to SCFA production, the unfractionated and 0.075 mm mango particles had significantly higher NH_3 concentrations than those for banana.

However, there was no significant difference between particle sizes for banana (*P*>0.05). The concentration of NH_3 production peaked between 8 and 18 h, and then declined. From 0 h, NH_3 concentrations of >2 mmol/g DM measured for both fruits suggests that some bacterial species within the porcine faecal microbiota have started actively fermenting some peptide/amino acid source present in the inoculum and/or medium.

Following the usual pattern for gut fermentation, acetic acid was the major SCFA produced (54-66%) in both fruits, followed by propionic (13-19%) and butyric acids (9-17%) (Fig 3), whereas valeric, isovaleric and isobutyric acids were minor SCFA, collectively accounting for <10%. These SCFA concentrations (mmol/g DM) were subsequently converted into acetic acid equivalents (AAE) (Table S1) using their respective molar mass to obtain a branched-chain ratio (BCR). The BCR gives an indication of the proportion of SCFA likely to be related to protein fermentation [4]. Banana fermentation was associated with a higher proportion of branched-chain SCFA (isobutyric, isovaleric and valeric acids) to straight chain acids (acetic, propionic and butyric acids), leading to a significantly higher BCR (*P*<0.0001) for banana than for mango.

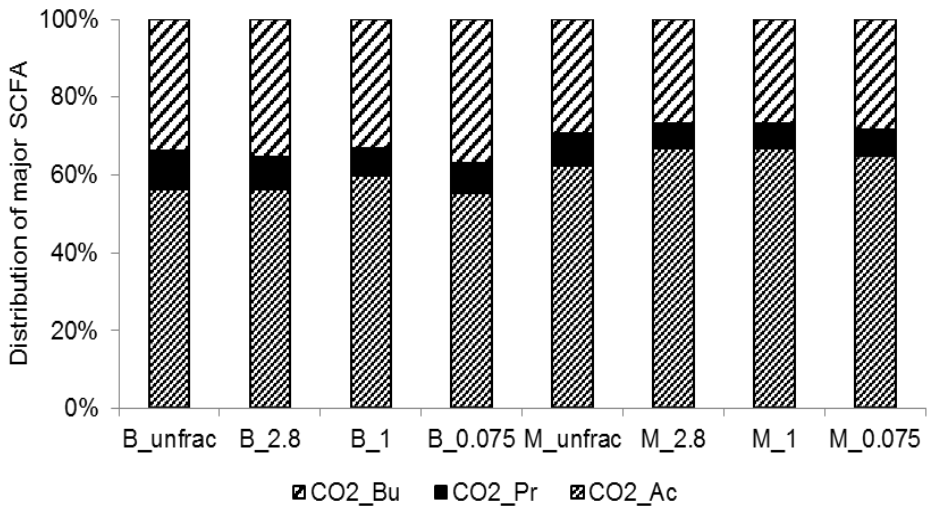

Figure 3. % Distribution of individual major short chain fatty acids (SCFA): acetic acid (Ac), propionic acid (Pr) and butyric acid (Bu) in mango and banana particles (n=4 for each particle size: unfractionated, 2.8 mm, 1 mm, 0.075 mm). M, mango; b, banana; CO_2, carbon dioxide.

2.3. Physical structures and major polysaccharide composition affecting fermentation

From confocal microscopy, it could be seen that masticated mango particles subjected to *in vitro* gastrointestinal digestion contained soft parenchyma (fleshy) tissue, which disappeared after microbial fermentation, leaving mostly cellulosic vascular fibres (Fig 4A).

This was confirmed by ^{13}CP/MAS NMR spectra of fermented 2.8 mm mango particles (Fig 5A) where the cellulose C-1 peak (dominant signal at 105 ppm [32, 33]) remained after fermentation, indicating that it was not well fermented. This is consistent with the micrographs (Fig 4A) where these vascular fibres are structured but loosely attached to the rest of the sample material. Vascular fibres were also present in banana after fermentation, but these were less pronounced than in mango, evidently thinner (Fig 4Cii), and were not resolved from more major peaks by NMR.

Banana particles after chewing and *in vitro* gastric and small intestinal digestion comprised mostly starch both before and after fermentation (Fig 5B). Before fermentation, starch granules were generally observed to be encapsulated by intact cell walls (Fig 4B). After fermentation, cell walls surrounding the starch were no longer detected, but liberated starch granules were still clearly visible (Fig 4Bii). This was supported by the solid state ^{13}C NMR spectra of samples both before and after fermentation showing a characteristic starch spectrum [34] including a C-1 peak, which overlapped with lower intensity cellulose signals (95-105 ppm). Evidence of partial fermentation of banana starch was observed using confocal microscopy, where the apparently roughened or scratched surfaces of the granule morphology is typical of the early stages of starch breakdown by amylolytic enzymes, as previously observed for both raw [35] and ripe bananas [36] and potato starch [37].

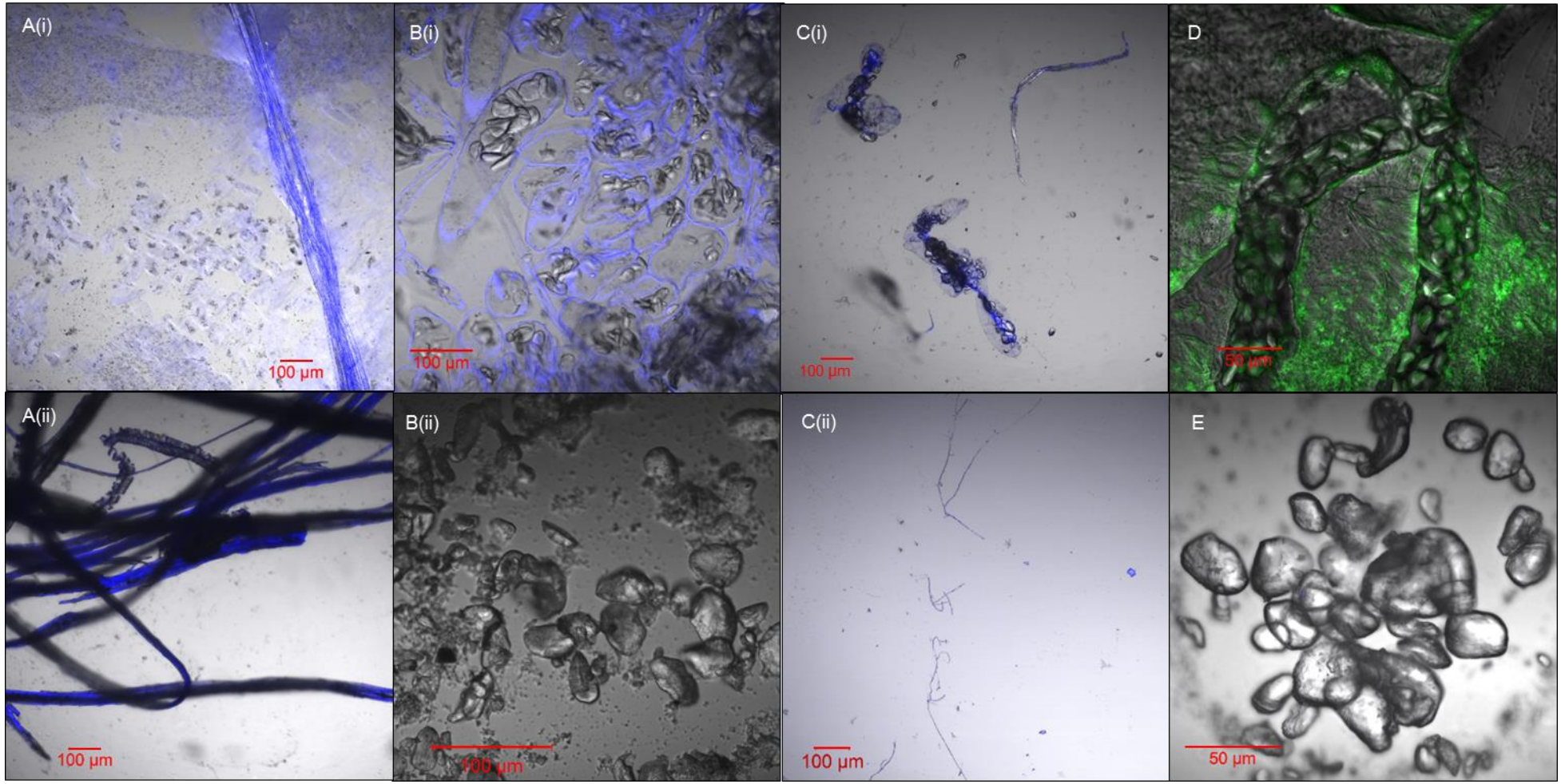

Figure 4. Differential interference contrast images of A(i) mango (2.8 mm), B(i) banana (2.8 mm) and C(i) banana (0.075 mm) cellular structures in blue fluorescence before microbial fermentation, and (D) banana starch granules (10-30 µm in length) in green fluorescence before fermentation. Thick cellulose vascular fibres remained in A(ii) mango after fermentation, whereas fermented banana comprised mostly of B(ii) starch and C(ii) some vascular fibres. Image (E) shows the rough and/or scratched surfaces of released banana starch granules after 48 h fermentation (63x magnification).

The ^{1}H NMR spectra (Fig 5C, 5D) indicated that pectic galactruonan was present in both mango and banana but this was not obvious in the ^{13}CP/MAS NMR spectra because of the overlap of the spinning side band (*ca* 99 ppm) from the carbonate peak (164 ppm) with the galacturonan C-1, which would appear from 98-101 ppm [33]. Rhamnose was present in mango as the major monosaccharide, which has been similarly reported in *Ataulfo* and *Tommy Atkins* cultivars [38], but was not observed in banana. Rhamnose, along with galacturonan residues were apparently utilised by the faecal microbiota, as they were not observed for either fruit after fermentation. Bacterial species capable of degrading pectin and/or cellulose in porcine faecal microbiota have been reported in numerous studies [39-41].

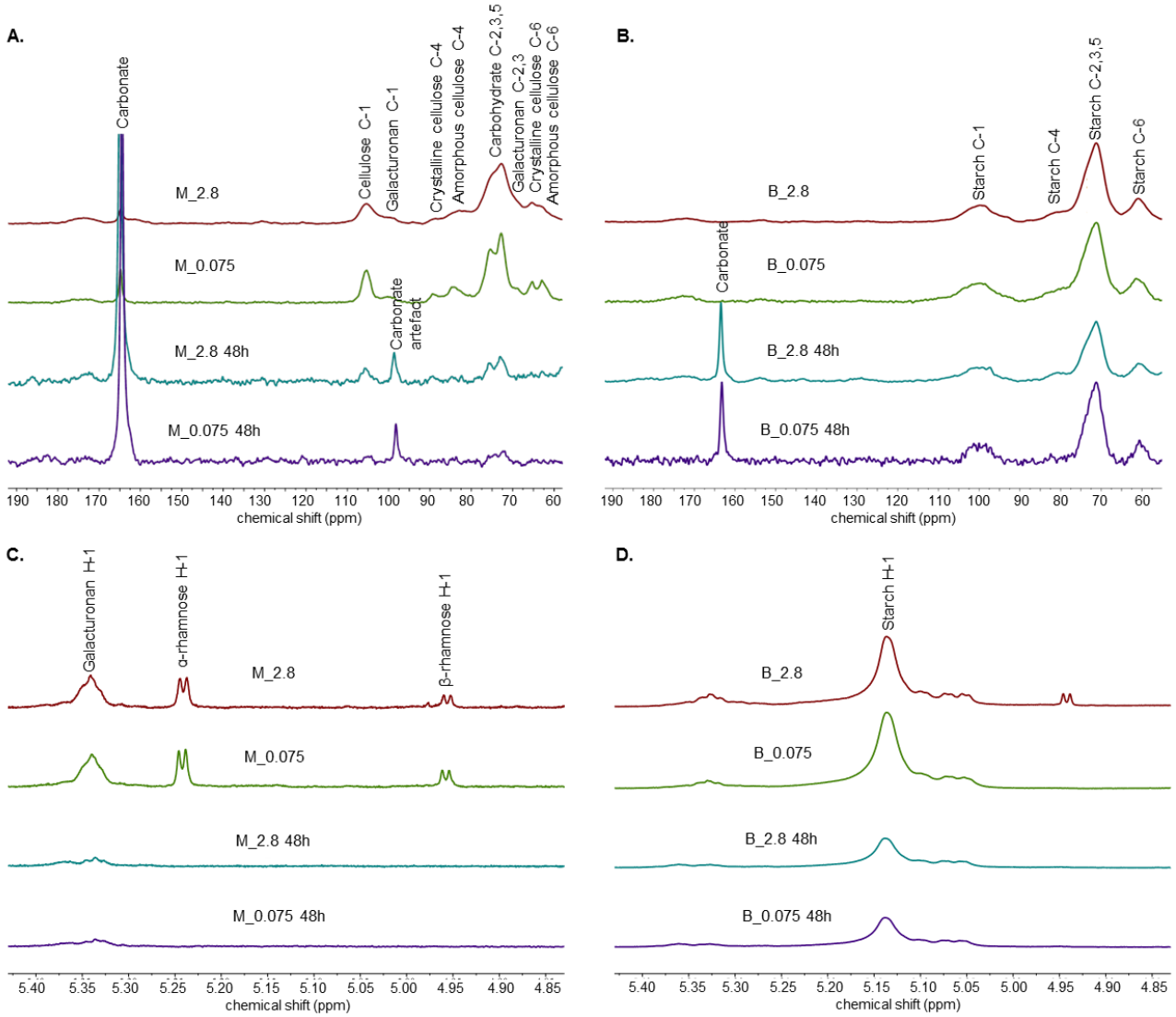

Figure 5. ^{13}CP/MAS and ^{1}H NMR spectra of masticated (A, C) mango and (B, D) banana particles of 2.8 mm and 0.075 mm respectively, before and after microbial fermentation (48 h). In (A) mango samples after fermentation, the chemical shift at 99 ppm is an artefactual spinning side band from the intense carbonate residue (164 ppm). The peaks at 105, 101, 89, 85, 69, 65 and 63 ppm are identified as cellulose C-1, galacturonan C-1, crystalline

cellulose C-4, amorphous cellulose C-4, crystalline C-6 and amorphous cellulose C-6 respectively [42]. The peaks at 72-77 ppm correspond to the C-2, 3, 5 of carbohydrates. In (B), the peaks at 105-95, 85-80 and 62 ppm are identified as C-1, C-4 and C-6 of starch, with C-2, 3, 5 of starch at 77-67 ppm [34]. In (C), the peaks before fermentation are assigned to anomeric protons of pectic galacturonan (5.4 ppm) [42], and monomeric rhamnose (5.24 and 4.96 ppm) [43]. The broad peak from 5.05-5.25 ppm in (D) banana is from anomeric protons of starch residues. M, mango; B, banana; 2.8 mm, 2.8 mm chewed fraction; 0.075, 0.075 mm chewed fraction. Results are consistent with monosaccharide analysis[44] after hydrolysis in either 1M H_2SO_4 (hydrolyses all polysaccharides except crystalline cellulose) and 12M H_2SO_4 (hydrolyses all polysaccharides), which showed that cellulose and 1M H_2SO_4 solubilised glucan (e.g. starch) were the main components present after fermentation of mango and banana respectively, with additional sugars characteristic of pectin and other cell wall components present before but to a lesser extent after fermentation.

3. Discussion

3.1. Effects of fruit and particle size on fermentation kinetics

Gas kinetics profiles showed significant differences between chewed mango and chewed banana both in terms of kinetics and end-points. Disintegration of the plant cell wall network and cell structures during *in vivo* mastication led to particles of varying sizes. The largest chewed fraction (2.8 mm) consisted of more fermentation-resistant cellulosic vascular tissues, whereas the 1 mm and 0.075 mm fractions contained mostly single cells and ruptured cell fragments, and little or no vascular fibres [26]. There was no significant particle size effect (P=0.43) on the cumulative gas production, however, there was a trend where the smaller mango particles of 0.075 mm were fermented more rapidly and extensively, and produced more gas (485 mL/g DM) than the larger (>1 mm) and unfractionated particles (411-445 mL/g DM). While decreasing particle size confers an expansion of surface area available for microbial accessibility and/or attachment [45, 46], the relative amount of vascular fibres is also a potential factor influencing this particle size effect. Fig 2 shows that the significant difference in surface area due to particle size was associated with kinetic rate (*i.e.* active fermentation) rather than lag (*i.e*. colonisation).

In contrast, the larger banana cell-cluster particles (2.8 mm) produced more gas (136 mL/g DM) than the smallest particles (0.075 mm) (93 mL/g DM). Larger banana particles may have contained a higher proportion of more fermentable cell wall structures. Similarly, in a previous study, multi-cellular carrot particles (137-298 μm) were fermented faster (23 mL/h) compared to 50-75 μm single carrot cells and fragments (8 mL/h) [6]. It appears that the plant cellular composition or architecture has a more significant impact than particle size or available surface area (exposed to the faecal microbiota). Fruit and vegetable matrices of varying physical and structural characteristics *i.e.* taproot or fruit, appeared to

have a strong influence on substrate fermentability, as did the cell contents. In this study, differences in substrate fermentability were due to a fruit effect, rather than a particle size effect, presumably due to the soft tissue structure of mango and banana.

3.2. Degradation of cell walls is more extensive than that of resistant starch

Chewed pieces of mango fruit were readily fermented as evidenced by the 48 h DMCV and SCFA values, leaving mostly long cellulosic vascular fibres after fermentation, which would be expected to be difficult to degrade by intestinal microbiota [47-49] depending on the chemical structure, microbial species and residence time in the gut [50]. The strands of cellulose in mango appeared not strongly connected to the parenchyma (fleshy) tissue, and were sometimes observed as separate strands before microbial fermentation, but clearly separated after fermentation. There appears to be a hierarchy in substrate utilisation as evidenced by the preferential degradation of (thinner) primary parenchyma cell walls over cellulosic vascular fibres.

Banana was far less efficiently fermented than mango, likely due to differences in their polysaccharide compositions. Cellulose was the major polysaccharide component of mango before and after fermentation (Figs 4A, 5A), while starch was the major component of banana before and after fermentation (Figs 4B, 5B). Starch granules encapsulated within intact banana cell walls survived mastication, as well as *in vitro* gastrointestinal digestion. The thin banana cell walls present before fermentation were apparently all fermented, releasing the starch granules that the cell walls had previously encapsulated. Most starch granules appeared smooth after mastication and 'digestion', but exhibited a parallel-striated surface after fermentation (Fig 4E). The fact that numerous and relatively intact starch granules were observed at the end of the fermentation shows that they were not rapidly fermented as soon as their encapsulating cell wall had been degraded. Indeed, banana starch in the granular form is relatively resistant to digestion by pancreatic enzymes [51], similar to other B-type starches such as potato. When treated with pancreatic amylases and amyloglucosidases *in vitro*, potato starch granules showed the same type of 'scratching' or exo-corrosion [37] as was found in the present study for banana starch granules after microbial fermentation. The smooth dense surface of (released) banana starch granules could also partially account for the intrinsic resistance of such granules to enzyme-catalysed hydrolysis by faecal microbiota. Additionally, banana starch has been previously reported to be highly resistant to *in vivo* human small intestinal digestion [52-54]. The thick external layer (several µm) of larger blockets [55], which surrounds the banana

granules, is composed of a hard and well organised material [51], and has been proposed to impede enzyme action and thus reduce hydrolysis rate. This same external layer can survive digestion of the granule interior giving rise to starch 'ghosts'[56], and it is possible that some residual starch is also in this form. Colonic bacteria reportedly utilise a Starch Utilisation System to reach these starch structures to extract glucose for energy [57], but the evidence from this study suggests colonic microbiota may not be any more effective than pancreatic amylases in overcoming the hard surface layer of banana starch granules.

Striations on the starch granule surface indicate the presence of microbial amylolytic activity in the fermentation medium, leading to erosion, but with limited hydrolytic effect. Some areas of the starch granule are more likely to be difficult to hydrolyse than other areas (crystalline regions appearing after partial hydrolysis) [35] and banana starch was described as having B-type crystallinity, which is typically associated with slow amylase digestion [58]. Additionally, during weighing of the masticated fractions into the fermentation bottles, it was noted that banana fractions had a more physically compact structure, which made it relatively difficult to obtain seemingly homogenous sub-samples. Accessibility, as influenced by the entrapping matrix of banana cells and/or cell clusters appeared to restrict access of the microbiota and/or their enzymes into the substrates.

3.3. Higher SCFA and NH_3 in mango but higher BCR in banana

Differences in SCFA and NH_3 between fruits were more pronounced than differences in particle sizes, where 68% and 64% significantly greater concentrations of SCFA and NH_3 respectively, were observed for mango as compared with banana ($P<0.0001$). This correlates well with the 74% greater $DMCV_{48}$ value for mango and is consistent with the expectation that more rapid and extensive fermentation is generally associated with higher SCFA production *in vitro* [59]. Particle size played a small role in SCFA production and had no significant effect on NH_3 production ($P>0.05$). Another fermentation study of wheat bran also found that finer wheat particles (50 μm) produced higher SCFA concentrations than larger clusters (758 μm) [60].

A lower total SCFA production typically corresponds to a proportionate increase in NH_3 levels. SCFA production in banana showed a lower total production, but there was no concomitant increase in NH_3, which was expected. Banana fermentation was associated with a higher BCR ($P<0.0001$), further validating the differences between these two fruits. Branched-chain SCFA are usually formed as a result of bacteria metabolising undigested

and endogenous proteins, peptides and amino acids, particularly when carbohydrates are in short supply as an energy source [13] or are difficult to utilise as found in this study. Here, NH_3 production was reduced for banana, which reflected the difference in availability of fermentable carbohydrate [39, 61], thus increasing the BCR.

The composition of dietary polysaccharides available for fermentation also influenced the proportions of SCFA produced. Resistant starch in banana appeared to favour an increased proportion of butyric acid (Fig 4), agreeing with previous reports that *in vitro* colonic fermentation of resistant starch is associated with elevated butyrate levels [62-64]. Conversely, the higher acetic acid % observed in mango can be ascribed to the presence of higher levels of cellulose and pectin, which is consistent with reported studies [65, 66] showing that acetate production predominates over propionate and butyrate in diets containing higher levels of non-starch polysaccharides.

4. Experimental

4.1. Preparation of fruit substrates

Fully ripe *Kensington Pride* mangoes and *Cavendish* bananas were procured from local stores in Brisbane, Queensland, Australia, two to three days before each of the three chewing sessions. The fruits were selected based on typical eating maturity, at stage 6 of mango ripeness (peel is yellow with a pink-red blush and flesh is slightly firm) [67] and stage 6 of banana ripeness (peel is completely yellow) [68]. Mangoes were stored at 4-6°C while bananas were stored at ambient temperature prior to the chewing sessions. The chewing selection and process, and bolus collection have been previously described [26]. From the twenty participants recruited, their expectorated boluses were collected and size fractionated, with each sieve fractions being weighed to obtain a % distribution of particle sizes ranging from >5.6 mm to 0.075 mm. This generated an individual mastication profile, allowing the participants to be categorised into various type of chewers. This profile was then used for the selection of a coarse chewer (with higher proportion of larger particle size fractions), in addition to another criterion: their consistency in producing a similar particle size distribution in each chewing experiment. In this study, a participant representing a coarse chewer was selected from the twenty participants and re-invited for three subsequent chewing sessions for bolus collection.

The fruits were first subjected to *in vivo* human mastication and wet-sieve fractionation (Fig 6) [26], followed by *in vitro* gastrointestinal digestion [6] and centrifugation at 3000 g for 10 min

(Avant®JE centrifuge, JA14 rotor). The pellets were then washed three times with water (1:3) to remove salivary components such as enzymes, soluble sugars and amino acids. Samples were stored at 4°C prior to *in vitro* microbial fermentation. The chewing experiment was approved by the Medical Research Ethics Committee at The University of Queensland (Ethical clearance no. 2012000683) and was performed in compliance with relevant laws and institutional guidelines. Participants gave informed consent to the experiment.

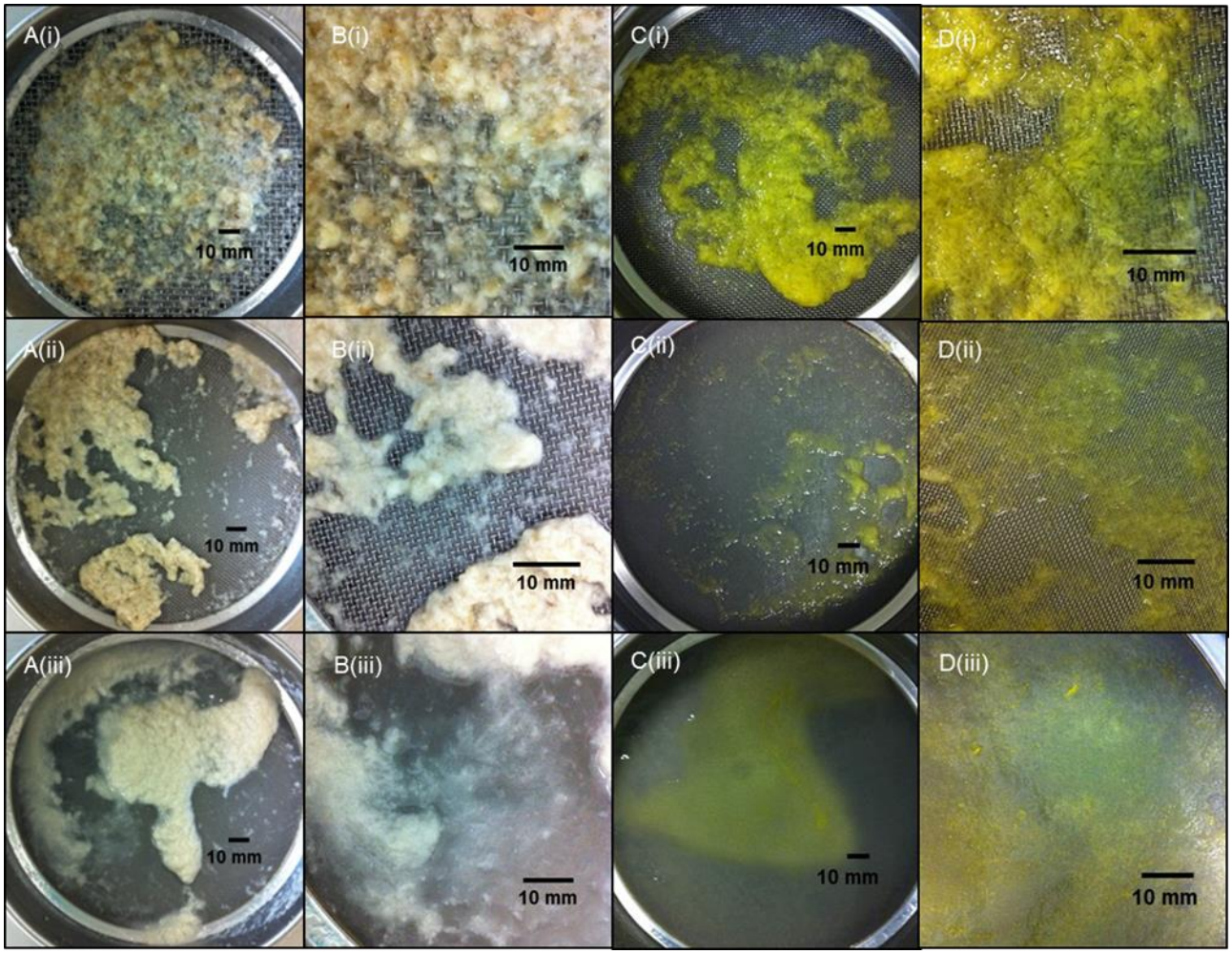

Figure 6. Images of masticated and fractionated (A & B) banana and (C & D) mango bolus particles captured on sieves of size (i) 2.8 mm, (ii) 1 mm and (iii) 0.075 mm. B(i-iii) and D(i-iii) show magnified views of each fraction respectively.

4.2. Preparation of faecal inoculum

Faecal inoculum was prepared as described previously [4]. Faeces were collected directly from five pigs (~35 kg) under ethics approval of the University of Queensland Animal Ethics Committee (SAFS/111/13/ARC). Prior to faecal collection, the pigs were fed a semi-purified diet based on highly digestible maize starch and fishmeal for ten days to avoid adaption of the gut microbiota to any of the substrates being used [69]. Faeces were kept in

pre-warmed CO_2-filled vacuum flasks during transport to the laboratory. To avoid (as far as possible) any effect of genetic variation of the pigs, the faeces from all five pigs were combined to make an inoculum representative of pigs as a whole. The faeces were then mixed (1:5) with pre-warmed saline (9 g/L NaCl), homogenised for 1 min under CO_2 and strained through four layers of muslin cloth within 2 h of faecal collection.

4.3. Cumulative gas production

The cumulative gas production technique was carried out as previously described [4]. Fresh unfractionated and fractionated mango (4.8±0.4 g) and banana (3.1±1.4 g) particles (each particle size, n=4), were weighed into 120 mL serum bottles containing 76 mL basal solution, 1 mL vitamin/phosphate buffer solution, 4 mL bicarbonate buffer and 1 mL reducing agent [70]. Unfractionated mango and banana refers to expectorated mango and banana boluses that were not sieved, containing mixed size particles. Faecal inoculum (4 mL) was added to each serum bottle and incubated at 39°C. Experimental blanks containing only inoculum and medium were also included. A steady stream of O_2-free CO_2 flowed into the fermentation bottles at all times prior to sealing with butyl rubber stoppers and aluminium crimp seals. The medium contained resazurin, known as an oxygen-reduction indicator, which did not turn pink, confirming there was no oxygen contamination in the bottles. Cumulative gas readings were measured using a pressure transducer (Type 453A, Bailey and Mackey Ltd., Birmingham, UK) and a LED digital readout voltmeter (Tracker 200) after insertion of a hypodermic syringe needle through the butyl rubber stopper above the fermentation solution. The head-space pressure and volume of gas were measured in each fermentation bottle (178 bottles) at 0, 2, 4, 6, 8, 10, 12, 15, 18, 21, 24, 27, 30, 33, 36, 39, 43, 46 and 48 h of the fermentation period according to the method of Williams et al. (2005) [4]. Then, the pressure and volume of gas recorded for each bottle was regressed to provide a corrected volume at each time per bottle. After cumulative gas readings were carried out for the bottles at their respective time intervals, they were placed immediately in iced-water to inhibit further microbial activity prior to sampling for post-fermentation analyses.

4.4. Post-fermentation analyses

pH of the fermentation solutions was recorded and aliquots were taken from all the fermentation time bottles at their respective time intervals for SCFA and NH_3 analyses. The remaining bottle contents were centrifuged at 4000 g for 10 min at 4°C and washed twice with water. Dry matter (DM) of the fermented samples (and substrates before

fermentation) was determined by drying to a constant weight at 103°C (ISO 6496, 1999) and then ashing by combustion at 550°C (ISO 5984, 1978).

SCFA in the fermented samples was extracted [72] with modifications to the microvacuum distillation apparatus (Fig 7), which has been expanded to distill 12 samples at one time. Sample aliquots (0.9 mL) and 1 M sulphuric acid (0.1 mL) containing 500 mM formic acid were added to the Thunberg tubes, frozen with liquid N_2 and vacuumed distilled. SCFA concentrations of the extracted aliquots were then analysed by gas chromatography using an Agilent GC-FID (HP6890) (Agilent Technologies, Mulgrave, VIC, Australia) and DB-FFAP capillary column (30 m x 0.5 mm) at a flow rate of 5.3 mL/min with helium as the carrier gas. Injector and detector temperatures were 250°C and oven temperature was programmed from 90°C (1 min) to 190°C (1 min) at 10°C/min). The injection volume was 0.5 µL. *Iso*-caproic acid was used as an internal standard. The SCFA mixed reference comprised of acetic acid (52.51 mM), propionic acid (13.4 mM), iso-butyric acid (1.07 mM), n-butyric acid (5.45 mM), iso-valeric acid (0.91 mM), n-valeric acid (0.92 mM), n-caproic acid (0.16 mM) and heptanoic acid (0.15 mM) (Sigma-Aldrich, Castle Hill, NSW, Australia). The BCR was calculated as the ratio of mainly branched chain acids (isobutyric, isovaleric and valeric acids- end-products of protein fermentation) concentration, to straight chain acids (acetic, propionic and butyric acids) that had all been corrected to mg of AAE using their respective molar masses.

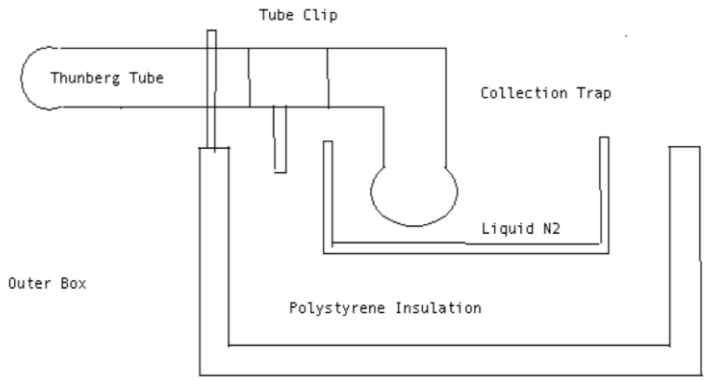

Figure 7. Simplified schematic diagram of vacuum distillation apparatus. An insulated box is constructed with a water-tight tray such that the Thunberg tube is held at a slight angle horizontally above the box by clips, which prevents liquid from running into the collection trap if the sample should melt. The bulb of the collection trap is in the open tray, which is filled with liquid N_2 so that the bulb is below the surface.

Analysis of NH_3 of the fermented samples involved a modified procedure [73]. Here, sample aliquots were mixed with 0.2 N HCl (1:1) with the concentrations of ammonium and

nitrogen being determined using the reduction of ammonium ions by sodium salicylate and nitroprusside in a weakly alkaline buffer (free chlorine). The resulting coloured complex was measured using a UV-Vis spectrophotometer (OlympusAU400, Tokyo, Japan) at 650 nm.

4.5. Nuclear magnetic resonance (NMR) spectroscopy

Solid-state ^{13}C CP/MAS NMR

Mango and banana particles, before and after fermentation (0 h and 48 h respectively), were freeze-dried and analysed by solid-state ^{13}C CP/MAS NMR spectroscopy using a Bruker MSL-300 spectrometer (Bruker, Karlsruhe, Germany) at a frequency of 75.46 MHz. Samples were lightly ground and stirred to ensure homogeneity, from which 200 mg was packed into a 4 mm diameter, cylindrical, PSZ (partially stabilized zirconium oxide) rotor with a KelF end cap. The rotor was spun at 5-6 kHz at the magic angle (54.7°). The 90° pulse width used was 5 µs, while a contact time of 1 ms and a recycle delay of 3 s was used for all samples. The spectral width was 38 kHz, acquisition time 50 ms, time domain points 2 k, transform size 4 k, and line broadening 50 Hz. At least 2400 scans were accumulated for each spectrum.

Solution state ^{1}H NMR

Similarly, freeze-dried mango and banana samples, before and after fermentation (0 h and 48 h respectively) (5 mg) were dissolved at 80°C overnight in 650 µL of d_6-DMSO containing 0.5 wt % LiBr. After the samples were cooled to room temperature, sodium 3-(trimethylsilyl)propionate-2,2,3,3-d4 (TSP) in D_2O was added as an internal standard. The addition of 50 µL of deuterated trifluoroacetic acid (d_1-TFA) directly before each measurement moved the HOD peak away from the diagnostic carbohydrate anomeric signals [74]. ^{1}H NMR spectra were measured on a Bruker Avance 500MHz spectrometer operating at 298K equipped with a 5 mm PABBO probe using 12 µs 90° pulse, 3.91 s acquisition time, 1 s relaxation delay and 64 scans.

4.6. Confocal laser scanning microscopy (CLSM)

Microscopy of mango and banana particles, before and after fermentation (0 h and 48 h respectively) was carried out using CLSM (LSM700, Carl Zeiss, Germany) under 10x and 40x objective lenses, differential interference contrast (DIC) and Zen (Black) 2011 software. Fluorescence of cell walls was observed at an excitation λ of 355 nm, emission λ from 400-440 nm, and laser power intensity of 2% after staining with Calcofluor. Starch

granules were stained with 3-aminopropyl-trimethoxysilane (APTS) followed by washing with 70% ethanol, incubating in APTS solution (10 mM APTS in 15% acetic acid) at 30°C overnight, washing five times with Milli-Q water and finally centrifuging at 3000 g for 10 min. Fluorescence of starch granules was observed at an excitation λ of 488 nm.

4.7. Curve fitting and statistical analysis

Cumulative gas production measured as a function of time was corrected to the volume (mL) of gas produced per g of substrate DM ($DMCV_{48}$) and was fitted to the monophasic Michaelis-Menten model [27] shown in Eq. (1):

$$DMCV_{48} = A/(1 + (C/t)^{B}) \quad (1)$$

where A is the asymptotic gas production (mL), B is the switching characteristic of the curve, C is the time at which half of the asymptotic value is reached ($T_{1/2}$) and t is the fermentation time (h). The maximal rate of gas production, R_{max} (mL/h) and the time at which it occurs, TR_{max} (h) were calculated from Eq. (2) and (3):

$$R_{max} = (A(CB)B(TR_{max}^{(-B-1)}))/(1+(C^{B})TR_{max}^{(-B)})^{2} \quad (2)$$

$$TR_{max} = C(((B-1)/(B+1))^{1/B}) \quad (3)$$

All parameters were tested for significant differences (effects of fruit, particle size and the interaction between fruit and particle size) using the Tukey-Kramer multiple comparison procedure as defined in Eq. (4):

$$Y = \mu + F_i + P_i + (F_i \times P_i) + \varepsilon_i \quad (4)$$

where Y is the dependent variable, μ is the mean, F_i is the effect of fruit, P_i is the effect of particle size, ($F_i \times P_i$) is the interaction between fruit and particle size, and ε_i is the error term. Statistical analyses were performed using SAS (9.3) NLIN (curve fitting) and GLM (significant difference) procedures [75].

5. Conclusions

The investigation of the fermentation characteristics of masticated particles of mango and banana has demonstrated distinct differences between the two fruits in terms of cellular architecture and starch content, which seemed to outweigh any effects of particle size on colonic-microbial fermentability. A decrease in particle size and a concomitant increase in available surface area would have been expected to increase the total gas production by

enhancing microbial accessibility. However, colonic fermentation differences between larger particle clusters (2.8-1 mm) and single cells or cell fragments (0.075 mm) were not as significant in the soft tissues of mango and banana studied here, as compared to a previous study on carrots with a more robust cellular structure [6]. The fruit (parenchyma) fleshy cells were fully or mostly fermented during fermentation, preferentially over resistant starch in banana, and over the thick cellulosic vascular fibres in mango. The slow fermentability of banana starch conferred by its intrinsic resistance and cell-wall encapsulation may have implications on calorific availability, satiety, glucose metabolism, and transit rates along the colon, and therefore deserves further study. The higher absolute levels of butyrate production from mango could be important in terms of contributing to anti-inflammatory and anti-carcinogenic properties [76-78] rather than the higher % ratio of butyrate to acetate/propionate in banana. Further studies investigating the extended fermentation of both fruits over 72 h and longer, and the microscopic degradation of banana cell walls with time, preferably 3-hourly should also be explored in future work.

6. Acknowledgements

The authors would like to thank Jelle Lahnstein (University of Adelaide) for monosaccharide analysis and the Australian Research Council Centre of Excellence in Plant Cell Walls for funding this study.

References

1. C. A. Edwards, G. Gibson, M. Champ, B. B. Jensen, J. C. Mathers, F. Nagengast, C. Rumney and A. Quehl, *J. Sci. Food Agric.*, 1996, 71, 209-217.
2. E. Bauer, B. A. Williams, C. Voigt, R. Mosenthin and M. W. A. Verstegen, *Arch. Anim. Nutr.*, 2010, 64, 394-411.
3. E. Bauer, B. A. Williams, C. Voigt, R. Mosenthin and M. W. A. Verstegen, *J. Sci. Food Agric.*, 2003, 83, 207-214.
4. B. A. Williams, M. W. Bosch, H. Boer, M. W. A. Verstegen and S. Tamminga, *Anim. Feed Sci. Technol.*, 2005, 123, 445-462.
5. S. Bazzocco, I. Mattila, S. Guyot, C. Renard and A. M. Aura, *Eur. J. Nutr.*, 2008, 47, 442-452.
6. L. Day, J. Gomez, S. K. Oiseth, M. J. Gidley and B. A. Williams, *J. Agric. Food Chem.*, 2012, 60, 3282-3290.
7. A. L. Molan, M. A. Lila, J. Mawson and S. De, *World J. Microbiol. Biotechnol.*, 2009, 25, 1243-1249.
8. M. H. Vong and M. L. Stewart, *Benef. Mirbobes*, 2013, 4, 291-295.
9. O. Piquer, C. Casado, S. Biglia, C. Fernandez, E. Blas and J. J. Pascual, *J. Anim. Feed Sci.*, 2009, 18, 743-757.
10. Z. S. Davies, D. Mason, A. E. Brooks, G. W. Griffith, R. J. Merry and M. K. Theodorou, *Anim. Feed Sci. Technol.*, 2000, 83, 205-221.
11. J. C. J. Groot, B. A. Williams, A. J. Oostdam, H. Boer and S. Tamminga, *British Journal of Nutrition*, 1998, 79, 519-525.
12. Y. T. Chiu and M. Stewart, *Journal of Medicinal Food*, 2012, 15, 120-125.
13. W. H. Hendriks, J. van Baal and G. Bosch, *Br. J. Nutr.*, 2012, 108, S247-S257.
14. R. Mosenthin, *Asian-Australasien Journal of Animal Science* 1998, 11, 608-619.
15. Y. S. Kim, J. K. Brecht and S. T. Talcott, *Food Chem.*, 2007, 105, 1327-1334.
16. M. W. Davey, J. Keulemans and R. Swennen, *J. Chromatogr. A*, 2006, 1136, 176-184.
17. H. Kim, J. Y. Moon, D. S. Lee, M. Cho, H. K. Choi, Y. S. Kim, A. Mosaddik and S. K. Cho, *Food Chem.*, 2010, 121, 429-436.
18. A. Z. Mercadante, D. B. Rodriguez-Amaya and G. Britton, *J. Agric. Food Chem.*, 1997, 45, 120-123.
19. C. M. Ajila, L. J. Rao and U. Rao, *Food Chem. Toxicol.*, 2010, 48, 3406-3411.
20. J. A. Manthey and P. Perkins-Veazie, *J. Agric. Food Chem.*, 2009, 57, 10825-10830.
21. J. D. Ornelas-Paz, E. M. Yahia and A. A. Gardea, *J. Agric. Food Chem.*, 2007, 55, 6628-6635.
22. R. M. Robles-Sanchez, H. Astiazaran-Garcia, O. Martin-Belloso, S. Gorinstein, E. Alvarez-Parrilla, L. A. d. l. Rosa, G. Yepiz-Plascencia and G. A. Gonzalez-Aguilar, *Food Research International*, 2011, 44, 1386-1391.
23. N. M. Shofian, A. A. Hamid, A. Osman, N. Saari, F. Anwar, M. S. P. Dek and R. Hairuddin, *Int. J. Mol. Sci.*, 2011, 12, 4678-4692.
24. J. Bouayed, L. Hoffmann and T. Bohn, *Food Chemistry: 128 (1) 14-21*, 2011, 128, 14-21.
25. M. Alothman, R. Bhat and A. A. Karim, *Food Chem.*, 2009, 115, 785-788.
26. D. Y. Low, B. D'Arcy and M. J. Gidley, *Food Research International*, 2015, 67, 238-246.
27. J. C. J. Groot, J. W. Cone, B. A. Williams, F. M. A. Debersaques and E. A. Lantinga, *Anim. Feed Sci. Technol.*, 1996, 64, 77-89.
28. P. J. Van Soest, *Nutritional ecology of the ruminant*, Cornell University Press, United States of America, 2nd edn., 1994.

29. H. J. Flint, K. P. Scott, S. H. Duncan, P. Louis and E. Forano, *Gut Microbes*, 2014, 3, 289-306.
30. J. M. Campbell, G. C. Fahey and B. W. Wolf, *J. Nutr.*, 1997, 127, 130-136.
31. S. Yanahira, M. Morita, S. Aoe, T. Suguri, Y. Takada, S. Miura and I. Nakajima, *J. Nutr. Sci. Vitaminol.*, 1997, 43, 123-132.
32. J. K. T. Ng, Z. D. Zujovic, B. G. Smith, J. W. Johnston, R. Schroder and L. D. Melton, *Carbohydr. Res.*, 2014, 386, 1-6.
33. M. Dick-Perez, Y. A. Zhang, J. Hayes, A. Salazar, O. A. Zabotina and M. Hong, *Biochemistry*, 2011, 50, 989-1000.
34. I. Tan, B. M. Flanagan, P. J. Halley, A. K. Whittaker and M. J. Gidley, *Biomacromolecules*, 2007, 8, 885-891.
35. P. Y. Zhang, R. L. Whistler, J. N. BeMiller and B. R. Hamaker, *Carbohydr. Polym.*, 2005, 59, 443-458.
36. K. Kayisu, L. F. Hood and P. J. Van soest, *J. Food Sci.*, 1981, 46, 1885-1890.
37. S. Dhital, A. K. Shrestha and M. J. Gidley, *Carbohydr. Polym.*, 2010, 82, 480-488.
38. M. D. Garcia-Magana, H. S. Garcia, L. A. Bello-Perez, S. G. Sayago-Ayerdi and M. M. M. de Oca, *Plant Food Hum. Nutr.*, 2013, 68, 254-258.
39. M. A. Sappok, W. F. Pellikaan, M. W. Verstegen, G. Bosch, A. Sundrum and W. H. Hendriks, *Journal of Science and Food Agriculture*, 2012, 93, 987-994.
40. B. A. Williams, M. W. Bosch, A. Awati, S. R. Konstantinov, H. Smidt, A. D. L. Akkermans, M. W. A. Verstegen and S. Tamminga, *Anim. Res.*, 2005, 54, 191-201.
41. F. Rink, E. Bauer, M. Eklund and R. Mosenthin, *Arch. Anim. Nutr.*, 2011, 65, 445-459.
42. C. M. G. C. Renard and M. C. Jarvis, *Plant Physiology*, 1999, 119, 1315-1322.
43. A. M. A. de Bruyn, R. de Gussem and G. G. S. Dutton, *Carbohydr. Res.*, 1976, 47, 158-163.
44. P. Comino, K. Shelat, H. Collins, J. Lahnstein and M. J. Gidley, *J. Agric. Food Chem.*, 2013, 61, 12111-12122.
45. J. Parada and J. M. Aguilera, *J. Food Sci.*, 2007, 72, 21-32.
46. F. Guillon, A. Auffret, J. A. Robertson, J. F. Thibault and J. L. Barry, *Carbohydr. Polym.*, 1998, 37, 185-197.
47. H. Yu, R. G. Liu, D. W. Shen, Y. Jiang and Y. Huang, *Polymer*, 2005, 46, 5689-5694.
48. F. Ismailbeigi, J. G. Reinhold, B. Faraji and P. Abadi, *J. Nutr.*, 1977, 107, 510-518.
49. S. Otles and S. Ozgoz, *Acta scientiarum polonorum. Technologia alimentaria*, 2014, 13, 191-202.
50. J. W. Anderson and W. J. L. Chen, *Am. J. Clin. Nutr.*, 1979, 32, 346-363.
51. C. A. Soares, F. H. G. Peroni-Okita, M. B. Cardoso, R. Shitakubo, F. M. Lajolo and B. R. Cordenunsi, *J. Agric. Food Chem.*, 2011, 59, 6672-6681.
52. N. Faisant, A. Buleon, P. Colonna, C. Molis, S. Lartigue, J. P. Galmiche and M. Champ, *Br. J. Nutr.*, 1995, 73, 111-123.
53. J. H. Cummings, E. R. Beatty, S. M. Kingman, S. A. Bingham and H. N. Englyst, *Br. J. Nutr.*, 1996, 75, 733-747.
54. H. N. Englyst and J. H. Cummings, *Am. J. Clin. Nutr.*, 1986, 44, 42-50.
55. N. Faisant, D. J. Gallant, B. Bouchet and M. Champ, *Eur. J. Clin. Nutr.*, 1995, 49, 98-104.
56. B. Zhang, S. Dhital, B. M. Flanagan and M. J. Gidley, *J. Agric. Food Chem.*, 2014, 62, 760-771.
57. E. C. Martens, N. M. Koropatkin, T. J. Smith and J. I. Gordon, *J. Biol. Chem.*, 2009, 284, 24673-24677.

58. B. R. Hamaker and Y. C. Tuncil, *Journal of Molecular Biology*, 2014, 426, 3838-3850.
59. D. L. Topping and P. M. Clifton, *Physiol. Rev.*, 2001, 81, 1031-1064.
60. D. J. A. Jenkins, C. W. C. Kendall, V. Vuksan, L. S. A. Augustin, Y. M. Li, B. Lee, C. C. Mehling, T. Parker, D. Faulkner, H. Seyler, E. Vidgen and V. Fulgoni, *J. Am. Coll. Nutr.*, 1999, 18, 339-345.
61. J. W. Cone, A. H. van Gelder and F. Driehuis, *Anim. Feed Sci. Technol.*, 1997, 66, 31-45.
62. D. J. Rose, A. Keshavarzian, J. A. Patterson, M. Venkatachalam, P. Gillevet and B. R. Hamaker, *Mol. Nutr. Food Res.*, 2009, 53, S121-S130.
63. J. L. J. Casterline, C. J. Oles and Y. Ku, *J. Agric. Food Chem.*, 1997, 45, 2463-2467.
64. U. Lehmann, G. Jacobasch and D. Schmiedl, *J. Agric. Food Chem.*, 2002, 50, 5236-5240.
65. G. Annison and D. L. Topping, *Annual Nutrition of review*, 1994, 14, 297-320.
66. A. G. Low, in *Recent developments in pig nutrition 2*, eds. D. J. A. Cole, W. Haresign and P. C. Garnsworthy, Nottingham University Press, Loughborough, Leicestershire, UK, 1993, ch. 11, pp. 137-162.
67. Primary Industries & Fisheries, Queensland Government, Queensland, Australia, 2012.
68. Isopan, Banana ripening, http://isopaninsulation.com/technologies/banana-ripening, Accessed August 3, 2011.
69. D. J. Wang, B. A. Williams, M. G. Ferruzzi and B. R. D'Arcy, *J. Sci. Food Agric.*, 2013, 93, 276-283.
70. S. E. Lowe, M. K. Theodorou, A. P. J. Trinci and R. B. Hespell, *J. Gen. Microbiol.*, 1985, 131, 2225-2229.
71. M. K. Theodorou, B. A. Williams, M. S. Dhanoa, A. B. McAllan and J. France, *Anim. Feed Sci. Technol.*, 1994, 48, 185-197.
72. H. J. Vreman, J. A. Dowling, R. A. Raubach and M. W. Weiner, *Anal. Chem.*, 1978, 50, 1138-1141.
73. W. E. Baethgen and M. M. Alley, *Commun. Soil Sci. Plant Anal.*, 1989, 20, 961-969.
74. M. J. Tizzotti, M. C. Sweedman, D. Tang, C. Schaefer and R. G. Gilbert, *J. Agric. Food Chem.*, 2011, 59, 6913-6919.
75. SAS, SAS Institute Inc., Cary, NC, USA, 9.3 edn., 2011.
76. M. A. R. Vinolo, H. G. Rodrigues, R. T. Nachbar and R. Curi, *Nutrients*, 2011, 3, 858-876.
77. S. Tedelind, F. Westberg, M. Kjerrulf and A. Vidal, *World Journal of Gastroenterology*, 2007, 13, 2826-2832.
78. E. A. Williams, J. M. Coxhead and J. C. Mathers, *Proc. Nutr. Soc.*, 2003, 62, 107-115.